Acta Cryst. (1999). B**55**, 410–423

The geometry and structural properties of the 4,8,12-trioxa-4,8,12,12c-tetrahydrodibenzo[*cd,mn*]pyrene system in the cationic state. Structures of a planar organic cation with various monovalent and divalent anions

Frederik C. Krebs,[a]* Bo W. Laursen,[a] Ib Johannsen,[a] André Faldt,[a] Klaus Bechgaard,[a] Claus S. Jacobsen,[b] Niels Thorup[c] and Kamal Boubekeur[d]

[a]*Condensed Matter Physics and Chemistry Department, Risø National Laboratory, DK-4000 Roskilde, Denmark,* [b]*Department of Physics, Technical University of Denmark, DK-2800 Lyngby, Denmark,* [c]*Department of Chemistry, Technical University of Denmark, DK-2800 Lyngby, Denmark, and* [d]*IMN, 2 rue de la Houssinière, 44072 Nantes, France. E-mail: frederik.krebs@risoe.dk*

(*Received 2 March 1998; accepted 30 November 1998*)

Abstract

The geometry of the 4,8,12-trioxa-4,8,12,12c-tetrahydrodibenzo[*cd*,*mn*]pyrene system in the cationic state was established by X-ray structural resolution of the salts formed between the cation and various anions. The geometry was found to be planar for the 4,8,12-trioxa-4,8,12,12c-tetrahydrodibenzo[*cd*,*mn*]pyrenylium and 2,6,10-tri(*tert*-butyl)-4,8,12-trioxa-4,8,12,12c-tetrahydrodibenzo[*cd*,*mn*]pyrenylium cations with the monovalent anions I^-, BF_4^-, PF_6^-, AsF_6^-, $HNO_3.NO_3^-$ and $CF_3SO_3^-$, and the divalent anions $S_2O_6^{2-}$ and $Mo_6Cl_{14}^{2-}$. The salts were found to crystallize in distinct space groups following a characteristic pattern. Mixed cation–anion stacking resulted in space groups with high symmetry: *Pbca* in three cases and $R\bar{3}c$ in one; a temperature study of the latter was made at ten different temperatures. The formation of dimers of anions and cations resulted in lower-symmetry space groups, mainly monoclinic ($P2_1/n$, $P2_1/c$ and $C2/c$), but also $P\bar{1}$.

1. Introduction

The 4,8,12-trioxa-4,8,12,12c-tetrahydrodibenzo[*cd*,*mn*]-pyrene system (1) has drawn much attention since it was first described by Martin & Smith (1964). The system has many interesting properties. When hydrogen or alkyl groups are attatched to the central C atom [position 12c (Panico *et al.* 1993)], the molecule may be considered to exhibit an attracting shape from the point of view of the design of cavitants and cryptants (Lofthagen *et al.*, 1991, 1992; Lofthagen & Siegel, 1995). Further interesting structural properties in the solid state have been described (Faldt *et al.*, 1997). When the central C atom in the 12c position is exchanged for a P atom, pyroelectric properties have been observed (Krebs *et al.*, 1997). Common to all the crystal structures reported in the literature is that the molecule is shaped like a Chinese hat, ideally with C_{3v} point symmetry.

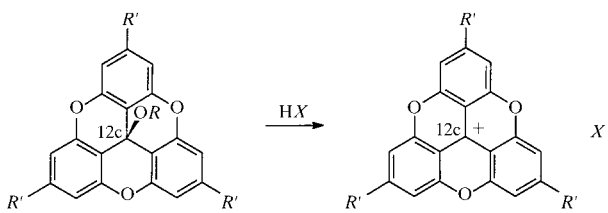

(1) $R=R'=$H
(2) $R=$Et, $R'=t$-Bu

(3) $R'=$H, $X=I^-$
(4) $R'=$H, $X=BF_4^-$
(5) $R'=$H, $X=AsF_6^-$
(6) $R'=$H, $X=PF_6^-$
(7) $R'=$H, $X=HNO_3{\cdot}NO_3^-$
(8) $R'=$H, $X=CF_3SO_3^-$
(9) $R'=$H, $X=Mo_6Cl_{14}^{2-}$
(10) $R'=$H, $X=S_2O_6^{2-}$
(11) $R'=t$-Bu, $X=PF_6^-, CH_3CN$
(12) $R'=t$-Bu, $X=Mo_6Cl_{14}^{2-}$

Electron spin resonance (ESR) studies of the free radical of the parent compound have shown that the radical molecules dimerize in solution (Sabacky *et al.*, 1967) and in one case the results gave indirect evidence of a planar conformation of the molecule in the radical form (Müller *et al.*, 1967).

In the cationic state the parent compound shows a remarkably high stability, which has been related to a postulated planar molecular structure (Martin & Smith, 1964), but until now no direct experimental evidence has been given for this.

In this paper we present the first direct evidence for the planarity of the cation of (1) from an X-ray crystallographic investigation of ten salts derived from the cations of (1) and (2). We identified characteristic classes of packing motifs depending on size, charge and symmetry of the constituents of the salts. Furthermore, a temperature study of one of the compounds was made at ten different temperatures.

Table 1. *Experimental details for (3), (4), (5), (6) at 120 K and (7)*

	(3)	(4)	(5)	(6) (120 K)	(7)
Crystal data					
Chemical formula	$C_{19}H_9O_3^+.I^-$	$C_{19}H_9O_3^+.BF_4^-$	$C_{19}H_9O_3^+.AsF_6^-$	$C_{19}H_9O_3^+.PF_6^-$	$C_{19}H_9O_3^+.NO_3^-.HNO_3$
Chemical formula weight	412.16	372.07	474.18	430.23	410.29
Cell setting	Orthorhombic	Orthorhombic	Orthorhombic	Trigonal	Monoclinic
Space group	*Pbca*	*Pbca*	*Pbca*	$R\bar{3}c$	$P2_1/n$
a (Å)	12.934 (3)	12.817 (3)	13.550 (3)	12.946 (2)	6.4960 (13)
b (Å)	14.748 (3)	15.196 (3)	15.807 (3)	–	7.6530 (15)
c (Å)	15.858 (3)	15.396 (3)	32.201 (6)	16.806 (3)	33.039 (7)
β (Å)	–	–	–	–	91.95 (3)
V (Å^3)	3024.9 (10)	2998.6 (10)	6897 (2)	2439.4 (7)	1641.5 (6)
Z	8	8	16	6	4
D_x (Mg m^{-3})	1.810	1.648	1.827	1.757	1.660
Radiation type	Mo $K\alpha$	Mo $K\alpha$	Mo $K\alpha$	Mo $K\alpha$	Mo $K\alpha$
Wavelength (Å)	0.7107	0.7107	0.7107	0.7107	0.7107
μ (mm^{-1})	2.129	0.143	2.053	0.256	0.136
Temperature (K)	293 (2)	120 (2)	293 (2)	120 (2)	120 (2)
Crystal form	Cube	Needle	Plate	Prism	Plate
Crystal size (mm)	0.32 × 0.30 × 0.30	0.45 × 0.25 × 0.10	0.30 × 0.23 × 0.18	0.25 × 0.25 × 0.075	0.43 × 0.18 × 0.05
Crystal colour	Dark red	Orange	Orange	Orange	Orange
Data collection					
Diffractometer	Siemens SMART CCD	Siemens SMART CCD	Siemens SMART CCD	Siemens SMART CCD	Siemens SMART CCD
Data collection method	ω scans	ω scans	ω scans	ω scans	ω scans
Absorption correction	Empirical (*SADABS*; Sheldrick, 1996)	Empirical (*SADABS*; Sheldrick, 1996)	Empirical (*SADABS*; Sheldrick, 1996)	None	Empirical (*SADABS*; Sheldrick, 1996)
T_{min}	0.476	0.871	0.404	–	0.776
T_{max}	0.603	0.980	0.603	–	0.980
No. of measured reflections	29370	29798	69140	8019	17025
No. of independent reflections	3093	3056	7003	557	3345
No. of observed reflections	2679	2381	4567	474	2173
Criterion for observed reflections	$I > 2\sigma(I)$	$I > 2\sigma(I)$	$I > 2\sigma(I)$	$I > 2\sigma(I)$	$I > 2\sigma(I)$
R_{int}	0.0250	0.0335	0.0743	0.0416	0.0622
θ_{max} (°)	26.37	26.36	26.32	26.32	26.33
Range of h, k, l	$-16 \rightarrow h \rightarrow 16$ $-18 \rightarrow k \rightarrow 18$ $-19 \rightarrow l \rightarrow 19$	$-16 \rightarrow h \rightarrow 16$ $-18 \rightarrow k \rightarrow 18$ $-19 \rightarrow l \rightarrow 19$	$-16 \rightarrow h \rightarrow 16$ $-19 \rightarrow k \rightarrow 19$ $-40 \rightarrow l \rightarrow 40$	$-16 \rightarrow h \rightarrow 16$ $-16 \rightarrow k \rightarrow 16$ $-20 \rightarrow l \rightarrow 20$	$-8 \rightarrow h \rightarrow 8$ $-9 \rightarrow k \rightarrow 9$ $-41 \rightarrow l \rightarrow 41$
Refinement					
Refinement on	F^2	F^2	F^2	F^2	F^2
$R[F^2>2\sigma(F^2)]$	0.0438	0.0437	0.0572	0.0261	0.0425
$wR(F^2)$	0.1104	0.1239	0.1779	0.0819	0.1134
S	1.196	1.031	1.068	1.047	1.002
No. of reflections used in refinement	3093	3054	7000	557	3345
No. of parameters used	209	244	523	47	271
H-atom treatment	Mixed	Mixed	Mixed	Mixed	Mixed
Weighting scheme	$w = 1/[\sigma^2(F_o^2) + (0.0552P)^2 + 2.1435P]$ where $P = (F_o^2 + 2F_c^2)/3$	$w = 1/[\sigma^2(F_o^2) + (0.0561P)^2 + 2.6840P]$ where $P = (F_o^2 + 2F_c^2)/3$	$w = 1/[\sigma^2(F_o^2) + (0.0824P)^2 + 14.1168P]$ where $P = (F_o^2 + 2F_c^2)/3$	$w = 1/[\sigma^2(F_o^2) + (0.0456P)^2 + 2.6625P]$ where $P = (F_o^2 + 2F_c^2)/3$	$w = 1/[\sigma^2(F_o^2) + (0.0549P)^2 + 0.5233P]$ where $P = (F_o^2 + 2F_c^2)/3$
$(\Delta/\sigma)_{max}$	0.003	−0.004	0.376	−0.002	0.002
$\Delta\rho_{max}$ (e Å^{-3})	0.383	0.562	1.046	0.185	0.219
$\Delta\rho_{min}$ (e Å^{-3})	−1.740	−0.517	−0.968	−0.301	−0.268
Extinction method	None	None	None	None	None

Table 1 (*cont.*)

	(3)	(4)	(5)	(6) (120 K)	(7)
Source of atomic scattering factors	*International Tables for Crystallography* (Vol. C)	*International Tables for Crystallography* (Vol. C)	*International Tables for Crystallography* (Vol. C)	*International Tables for Crystallography* (Vol. C)	*International Tables for Crystallography* (Vol. C)
Computer programs					
Data collection	*SMART* (Siemens, 1995)	*SMART* (Siemens, 1995)	*SMART* (Siemens, 1995)	*SMART* (Siemens, 1995)	*SMART* (Siemens, 1995)
Cell refinement	*SAINT* (Siemens, 1995)	*SAINT* (Siemens, 1995)	*SAINT* (Siemens, 1995)	*SAINT* (Siemens, 1995)	*SAINT* (Siemens, 1995)
Data reduction	*SAINT* (Siemens, 1995)	*SAINT* (Siemens, 1995)	*SAINT* (Siemens, 1995)	*SAINT* (Siemens, 1995)	*SAINT* (Siemens, 1995)
Structure solution	*SHELXS*86 (Sheldrick, 1990)	*SHELXS*86 (Sheldrick, 1990)	*SHELXS*86 (Sheldrick, 1990)	*SHELXS*86 (Sheldrick, 1990)	*SHELXS*97 (Sheldrick, 1990)
Structure refinement	*SHELXL*93 (Sheldrick, 1993)	*SHELXL*93 (Sheldrick, 1993)	*SHELXL*93 (Sheldrick, 1993)	*SHELXL*93 (Sheldrick, 1993)	*SHELXL*97 (Sheldrick, 1997)
Preparation of material for publication	*XCIF* (Sheldrick, 1993)	*XCIF* (Sheldrick, 1993)	*XCIF* (Sheldrick, 1993)	*XCIF* (Sheldrick, 1993)	*XCIF* (Sheldrick, 1993)

Table 2. *Experimental details for (8), (9), (10), (11) and (12)*

	(8)	(9)	(10)	(11)	(12)
Crystal data					
Chemical formula	$C_{19}H_9O_3^+.CF_3SO_3^-$	$C_{19}H_9O_3^+.0.5Mo_6Cl_{14}^{2-}$	$C_{19}H_9O_3^+.0.5S_2O_6^{2-}$	$C_{31}H_{33}O_3^+.PF_6^-.CH_3CN$	$C_{31}H_{33}O_3^+.0.5Mo_6Cl_{14}^{2-}$
Chemical formula weight	434.33	821.23	365.32	639.6	989.54
Cell setting	Monoclinic	Monoclinic	Triclinic	Monoclinic	Monoclinic
Space group	$P2_1/c$	$C2/c$	$P\overline{1}$	$P2_1/n$	$P2_1/n$
a (Å)	15.771 (3)	18.205 (4)	8.6300 (17)	12.085 (2)	17.157 (3)
b (Å)	15.473 (3)	13.540 (3)	8.9680 (18)	11.347 (2)	11.130 (2)
c (Å)	15.332 (3)	18.679 (4)	9.876 (2)	22.930 (5)	18.456 (4)
α (°)	–	–	97.91 (3)	–	–
β (°)	115.70 (3)	97.93 (3)	102.37 (3)	102.87 (3)	96.40 (3)
γ (°)	—	—	108.61 (3)	—	—
V (Å^3)	3371.3 (12)	4560.3 (16)	689.8 (2)	3065.4 (11)	3502.4 (12)
Z	8	8	2	4	4
D_x (Mg m^{-3})	1.711	2.392	1.759	1.386	1.877
Radiation type	Mo $K\alpha$	Mo $K\alpha$	Mo $K\alpha$	Mo $K\alpha$	Mo $K\alpha$
Wavelength (Å)	0.7107	0.7107	0.7107	0.7107	0.7107
μ (mm^{-1})	0.265	2.468	0.276	0.162	1.624
Temperature (K)	120 (2)	120 (2)	120 (2)	120 (2)	120 (2)
Crystal form	Plate	Prism	Plate	Plate	Cube
Crystal size (mm)	0.45 × 0.30 × 0.23	0.18 × 0.13 × 0.10	0.50 × 0.33 × 0.20	0.48 × 0.40 × 0.15	0.28 × 0.20 × 0.20
Crystal colour	Orange	Orange	Orange	Orange	Orange
Data collection					
Diffractometer	Siemens SMART CCD	Siemens SMART CCD	Siemens SMART CCD	Siemens SMART CCD	Siemens SMART CCD
Data collection method	ω scans	ω scans	ω scans	ω scans	ω scans
Absorption correction	Empirical (*SADABS*; Sheldrick, 1996)	Empirical (*SADABS*; Sheldrick, 1996)	Empirical (*SADABS*; Sheldrick, 1996)	Empirical (*SADABS*; Sheldrick, 1996)	Empirical (*SADABS*; Sheldrick, 1996)
T_{min}	0.713	0.776	0.616	0.853	0.704
T_{max}	0.928	0.862	0.962	0.978	0.886
No. of measured reflections	35210	23431	5953	31555	36072
No. of independent reflections	6860	4631	2779	6252	7149
No. of observed reflections	5770	4029	2452	5092	6258
Criterion for observed reflections	$I > 2\sigma(I)$	$I > 2\sigma(I)$	$I > 2\sigma(I)$	$I > 2\sigma(I)$	$I > 2\sigma(I)$
R_{int}	0.0301	0.0297	0.0189	0.0254	0.0271

Table 2 (*cont.*)

	(8)	(9)	(10)	(11)	(12)
θ_{max} (°)	26.33	26.32	26.37	26.36	26.37
Range of h, k, l	$-19 \rightarrow h \rightarrow 19$ $-19 \rightarrow k \rightarrow 19$ $-19 \rightarrow l \rightarrow 19$	$-22 \rightarrow h \rightarrow 22$ $-16 \rightarrow k \rightarrow 16$ $-23 \rightarrow l \rightarrow 23$	$-10 \rightarrow h \rightarrow 10$ $-11 \rightarrow k \rightarrow 11$ $-12 \rightarrow l \rightarrow 12$	$-15 \rightarrow h \rightarrow 15$ $-14 \rightarrow k \rightarrow 14$ $-28 \rightarrow l \rightarrow 28$	$-21 \rightarrow h \rightarrow 21$ $-13 \rightarrow k \rightarrow 13$ $-23 \rightarrow l \rightarrow 23$
Refinement					
Refinement on	F^2	F^2	F^2	F^2	F^2
$R[F^2>2\sigma(F^2)]$	0.0315	0.0221	0.0323	0.0363	0.0235
$wR(F^2)$	0.0889	0.0563	0.0923	0.0997	0.0582
S	1.022	1.094	1.024	1.043	1.097
No. of reflections used in refinement	6860	4631	2779	6252	7149
No. of parameters used	541	289	235	434	397
H-atom treatment	Mixed	Mixed	Mixed	Mixed	Mixed
Weighting scheme	$w = 1/[\sigma^2(F_o^2) + (0.0524P)^2 + 1.1788P]$ where $P = (F_o^2 + 2F_c^2)/3$	$w = 1/[\sigma^2(F_o^2) + (0.0310P)^2 + 4.5834P]$ where $P = (F_o^2 + 2F_c^2)/3$	$w = 1/[\sigma^2(F_o^2) + (0.0629P)^2 + 0.1004P]$ where $P = (F_o^2 + 2F_c^2)/3$	$w = 1/[\sigma^2(F_o^2) + (0.0441P)^2 + 1.7107P]$ where $P = (F_o^2 + 2F_c^2)/3$	$w = 1/[\sigma^2(F_o^2) + (0.0303P)^2 + 1.6569P]$ where $P = (F_o^2 + 2F_c^2)/3$
$(\Delta/\sigma)_{max}$	−0.002	0.01	0.002	0.054	0.005
$\Delta\rho_{max}$ (e Å^{-3})	0.318	0.379	0.439	0.275	0.432
$\Delta\rho_{min}$ (e Å^{-3})	−0.537	−1.210	−0.500	−0.386	−1.313
Extinction method	None	None	None	None	None
Source of atomic scattering factors	*International Tables for Crystallography* (Vol. C)	*International Tables for Crystallography* (Vol. C)	*International Tables for Crystallography* (Vol. C)	*International Tables for Crystallography* (Vol. C)	*International Tables for Crystallography* (Vol. C)
Computer programs					
Data collection	*SMART* (Siemens, 1995)	*SMART* (Siemens, 1995)	*SMART* (Siemens, 1995)	*SMART* (Siemens, 1995)	*SMART* (Siemens, 1995)
Cell refinement	*SAINT* (Siemens, 1995)	*SAINT* (Siemens, 1995)	*SAINT* (Siemens, 1995)	*SAINT* (Siemens, 1995)	*SAINT* (Siemens, 1995)
Data reduction	*SAINT* (Siemens, 1995)	*SAINT* (Siemens, 1995)	*SAINT* (Siemens, 1995)	*SAINT* (Siemens, 1995)	*SAINT* (Siemens, 1995)
Structure solution	*SHELXS*86 (Sheldrick, 1990)	*SHELXS*97 (Sheldrick, 1990)	*SHELXS*97 (Sheldrick, 1990)	*SHELXS*97 (Sheldrick, 1990)	*SHELXS*97 (Sheldrick, 1990)
Structure refinement	*SHELXL*93 (Sheldrick, 1993)	*SHELXL*97 (Sheldrick, 1997)	*SHELXL*97 (Sheldrick, 1997)	*SHELXL*97 (Sheldrick, 1997)	*SHELXL*97 (Sheldrick, 1997)
Preparation of material for publication	*XCIF* (Sheldrick, 1993)	*XCIF* (Sheldrick, 1993)	*XCIF* (Sheldrick, 1993)	*XCIF* (Sheldrick, 1993)	*XCIF* (Sheldrick, 1993)

2. Experimental

2.1. *Preparation methods*

All reagents used were standard grade unless otherwise stated. The crystals used for X-ray crystallography were obtained from HPLC grade solvents. Compound (1) was prepared as described by Martin & Smith (1964). Compound (2) and the salts (6) and (11) were prepared as described by Faldt *et al.* (1997). Compounds (3), (4), (5), (7) and (8) were prepared by adding a slight excess of the corresponding acid to a solution of (1) in tetrahydrofuran (thf). The precipitate was filtered and washed with thf and recrystallized by dissolution in acetonitrile followed by addition of ethyl acetate. Slow evaporation of the mixture yielded the crystals used for X-ray structure determination. In the case of the iodine salt, (3), the crystallization was repeated twice. For compound (10), for which the acid was not commercially available, the acid was prepared *in situ* by reaction of the sodium salt of the corresponding acid with hydrochloric acid. Crystallization was carried out in water. Compound (11) crystallizes with one acetonitrile solvent molecule per formula unit, which was lost upon drying the crystals. Compounds (9) and (12) were prepared by *in situ* formation of the molybdenum cluster followed by the addition of (1) or (2); a description of the preparation of (12) follows as an example.

$MoCl_2$ (0.38 g, 3 mmol) was dissolved in boiling ethanol (25 ml) and filtered to remove any insoluble impurities. HCl in ethanol (0.2 ml, 8 *M*) was added to the yellow solution followed by compound (2) (0.24 g, 0.4 mmol) in toluene/ethanol (1:1) (25 ml). The orange crystals of (12) were collected, washed and dried. The yield was near quantitative. Recrystallization from acetonitrile/dimethylformamide (5:1) yielded large orange crystals, used for X-ray structure determination.

Melting points were determined using a BÜCHI 510 melting-point apparatus. The melting points of compounds (3), (4), (5), (8), (9), (10) and (12) are above 573 K. For compound (7) melting takes place with

Table 3. *Experimental details for (6) at 160, 198, 220, 243 and 268 K*

	(6) (160 K)	(6) (198 K)	(6) (220 K)	(6) (243 K)	(6) (268 K)
Crystal data					
Chemical formula	$C_{19}H_9O_3^+.PF_6^-$	$C_{19}H_9O_3^+.PF_6^-$	$C_{19}H_9O_3^+.PF_6^-$	$C_{19}H_9O_3^+.PF_6^-$	$C_{19}H_9O_3^+.PF_6^-$
Chemical formula weight	430.23	430.23	430.23	430.23	430.23
Cell setting	Trigonal	Trigonal	Trigonal	Trigonal	Trigonal
Space group	$R\bar{3}c$	$R\bar{3}c$	$R\bar{3}c$	$R\bar{3}c$	$R\bar{3}c$
a (Å)	12.964 (2)	12.997 (2)	13.015 (2)	13.040 (2)	13.067 (2)
c (Å)	16.813 (3)	16.843 (3)	16.859 (3)	16.884 (3)	16.910 (3)
V (Å^3)	2447.3 (7)	2464.0 (7)	2473.3 (7)	2486.5 (7)	2500.4 (7)
Z	6	6	6	6	6
D_x (Mg m^{-3})	1.752	1.740	1.733	1.724	1.714
Radiation type	Mo $K\alpha$	Mo $K\alpha$	Mo $K\alpha$	Mo $K\alpha$	Mo $K\alpha$
Wavelength (Å)	0.7107	0.7107	0.7107	0.7107	0.7107
μ (mm^{-1})	0.255	0.253	0.252	0.251	0.25
Temperature (K)	160 (2)	198 (2)	220 (2)	243 (2)	268 (2)
Crystal form	Prism	Prism	Prism	Prism	Prism
Crystal size (mm)	0.25 × 0.25 × 0.075	0.25 × 0.25 × 0.075	0.25 × 0.25 × 0.075	0.25 × 0.25 × 0.075	0.25 × 0.25 × 0.075
Crystal colour	Orange	Orange	Orange	Orange	Orange
Data collection					
Diffractometer	Siemens SMART CCD	Siemens SMART CCD	Siemens SMART CCD	Siemens SMART CCD	Siemens SMART CCD
Data collection method	ω scans	ω scans	ω scans	ω scans	ω scans
Absorption correction	None	None	None	None	None
No. of measured reflections	8102	8165	8196	8207	8252
No. of independent reflections	561	566	567	569	572
No. of observed reflections	425	397	380	352	352
Criterion for observed reflections	$I > 2\sigma(I)$	$I > 2\sigma(I)$	$I > 2\sigma(I)$	$I > 2\sigma(I)$	$I > 2\sigma(I)$
R_{int}	0.0520	0.0567	0.0570	0.0605	0.0621
θ_{max} (°)	26.36	26.36	26.36	26.36	26.35
Range of h, k, l	$-16 \rightarrow h \rightarrow 16$ $-15 \rightarrow k \rightarrow 16$ $-21 \rightarrow l \rightarrow 21$	$-16 \rightarrow h \rightarrow 16$ $-16 \rightarrow k \rightarrow 15$ $-21 \rightarrow l \rightarrow 21$	$-16 \rightarrow h \rightarrow 16$ $-16 \rightarrow k \rightarrow 16$ $-21 \rightarrow l \rightarrow 21$	$-16 \rightarrow h \rightarrow 16$ $-16 \rightarrow k \rightarrow 15$ $-21 \rightarrow l \rightarrow 21$	$-16 \rightarrow h \rightarrow 16$ $-16 \rightarrow k \rightarrow 16$ $-21 \rightarrow l \rightarrow 21$
Refinement					
Refinement on	F^2	F^2	F^2	F^2	F^2
$R[F^2>2\sigma(F^2)]$	0.0310	0.0333	0.0325	0.0296	0.0371
$wR(F^2)$	0.0902	0.0988	0.0993	0.0953	0.1124
S	1.036	1.060	1.022	0.948	1.067
No. of reflections used in refinement	561	566	566	569	571
No. of parameters used	47	47	47	47	47
Weighting scheme	$w = 1/[\sigma^2(F_o^2) + (0.0456P)^2 + 2.6625P]$ where $P = (F_o^2 + 2F_c^2)/3$	$w = 1/[\sigma^2(F_o^2) + (0.0456P)^2 + 2.6625P]$ where $P = (F_o^2 + 2F_c^2)/3$	$w = 1/[\sigma^2(F_o^2) + (0.0456P)^2 + 2.6625P]$ where $P = (F_o^2 + 2F_c^2)/3$	$w = 1/[\sigma^2(F_o^2) + (0.0456P)^2 + 2.6625P]$ where $P = (F_o^2 + 2F_c^2)/3$	$w = 1/[\sigma^2(F_o^2) + (0.0456P)^2 + 2.6625P]$ where $P = (F_o^2 + 2F_c^2)/3$
$(\Delta/\sigma)_{max}$	−0.007	0.011	−0.01	−0.023	−0.04
$\Delta\rho_{max}$ (e Å^{-3})	0.178	0.140	0.147	0.145	0.116
$\Delta\rho_{min}$ (e Å^{-3})	−0.298	−0.267	−0.300	−0.201	−0.190
Extinction method	None	None	None	None	None
Source of atomic scattering factors	*International Tables for Crystallography* (Vol. C)	*International Tables for Crystallography* (Vol. C)	*International Tables for Crystallography* (Vol. C)	*International Tables for Crystallography* (Vol. C)	*International Tables for Crystallography* (Vol. C)
Computer programs					
Data collection	*SMART* (Siemens, 1995)	*SMART* (Siemens, 1995)	*SMART* (Siemens, 1995)	*SMART* (Siemens, 1995)	*SMART* (Siemens, 1995)

Table 3 (*cont.*)

	(6) (160 K)	(6) (198 K)	(6) (220 K)	(6) (243 K)	(6) (268 K)
Cell refinement	*SAINT* (Siemens, 1995)	*SAINT* (Siemens, 1995)	*SAINT* (Siemens, 1995)	*SAINT* (Siemens, 1995)	*SAINT* (Siemens, 1995)
Data reduction	*SAINT* (Siemens, 1995)	*SAINT* (Siemens, 1995)	*SAINT* (Siemens, 1995)	*SAINT* (Siemens, 1995)	*SAINT* (Siemens, 1995)
Structure solution	*SHELXS*86 (Sheldrick, 1990)	*SHELXS*86 (Sheldrick, 1990)	*SHELXS*86 (Sheldrick, 1990)	*SHELXS*86 (Sheldrick, 1990)	*SHELXS*86 (Sheldrick, 1990)
Structure refinement	*SHELXL*93 (Sheldrick, 1993)	*SHELXL*93 (Sheldrick, 1993)	*SHELXL*93 (Sheldrick, 1993)	*SHELXL*93 (Sheldrick, 1993)	*SHELXL*93 (Sheldrick, 1993)
Preparation of material for publication	*XCIF* (Sheldrick, 1993)	*XCIF* (Sheldrick, 1993)	*XCIF* (Sheldrick, 1993)	*XCIF* (Sheldrick, 1993)	*XCIF* (Sheldrick, 1993)

Table 4. *Experimental details for (6) at 293, 313, 338 and 373 K*

	(6) (293 K)	(6) (313 K)	(6) (338 K)	(6) (373 K)
Crystal data				
Chemical formula	$C_{19}H_9O_3^+.PF_6^-$	$C_{19}H_9O_3^+.PF_6^-$	$C_{19}H_9O_3^+.PF_6^-$	$C_{19}H_9O_3^+.PF_6^-$
Chemical formula weight	430.23	430.23	430.23	430.23
Cell setting	Trigonal	Trigonal	Trigonal	Trigonal
Space group	$R\bar{3}c$	$R\bar{3}c$	$R\bar{3}c$	$R\bar{3}c$
a (Å)	13.094 (2)	13.111 (2)	13.131 (2)	13.181 (2)
c (Å)	16.937 (3)	16.953 (3)	16.970 (3)	17.025 (3)
V (Å^3)	2514.7 (7)	2523.6 (7)	2534.0 (7)	2561.6 (7)
Z	6	6	6	6
D_x (Mg m^{-3})	1.705	1.699	1.692	1.673
Radiation type	Mo $K\alpha$	Mo $K\alpha$	Mo $K\alpha$	Mo $K\alpha$
Wavelength (Å)	0.71073	0.71073	0.71073	0.71073
μ (mm^{-1})	0.248	0.247	0.246	0.244
Temperature (K)	293 (2)	313 (2)	338 (2)	373 (2)
Crystal form	Prism	Prism	Prism	Prism
Crystal size (mm)	0.25 × 0.25 × 0.075	0.25 × 0.25 × 0.075	0.25 × 0.25 × 0.075	0.25 × 0.25 × 0.075
Crystal colour	Orange	Orange	Orange	Orange
Data collection				
Diffractometer	Siemens SMART CCD	Siemens SMART CCD	Siemens SMART CCD	Siemens SMART CCD
Data collection method	ω scans	ω scans	ω scans	ω scans
Absorption correction	None	None	None	None
No. of measured reflections	8328	8369	8356	8443
No. of independent reflections	575	577	579	586
No. of observed reflections	310	303	275	249
Criterion for observed reflections	$I > 2\sigma(I)$	$I > 2\sigma(I)$	$I > 2\sigma(I)$	$I > 2\sigma(I)$
R_{int}	0.0669	0.0667	0.0708	0.0801
θ_{max} (°)	26.36	26.34	26.39	26.34
Range of h, k, l	$-16 \rightarrow h \rightarrow 16$ $-16 \rightarrow k \rightarrow 16$ $-21 \rightarrow l \rightarrow 21$	$-16 \rightarrow h \rightarrow 16$ $-16 \rightarrow k \rightarrow 16$ $-21 \rightarrow l \rightarrow 21$	$-16 \rightarrow h \rightarrow 16$ $-16 \rightarrow k \rightarrow 15$ $-21 \rightarrow l \rightarrow 21$	$-16 \rightarrow h \rightarrow 16$ $-16 \rightarrow k \rightarrow 15$ $-21 \rightarrow l \rightarrow 21$
Refinement				
Refinement on	F^2	F^2	F^2	F^2
$R[F^2>2\sigma(F^2)]$	0.0344	0.0363	0.0365	0.0420
$wR(F^2)$	0.1106	0.1095	0.1137	0.1276
S	1.001	1.054	1.049	1.093
No. of reflections used in refinement	575	576	579	586
No. of parameters used	47	47	47	47
Weighting scheme	$w = 1/[\sigma^2(F_o^2) + (0.0456P)^2 + 2.6625P]$ where $P = (F_o^2 + 2F_c^2)/3$	$w = 1/[\sigma^2(F_o^2) + (0.0454P)^2 + 1.2721P]$ where $P = (F_o^2 + 2F_c^2)/3$	$w = 1/[\sigma^2(F_o^2) + (0.0454P)^2 + 1.2721P]$ where $P = (F_o^2 + 2F_c^2)/3$	$w = 1/[\sigma^2(F_o^2) + (0.0454P)^2 + 1.2721P]$ where $P = (F_o^2 + 2F_c^2)/3$
$(\Delta/\sigma)_{max}$	−0.022	0.003	−0.028	0.078
$\Delta\rho_{max}$ (e Å^{-3})	0.115	0.104	0.113	0.154
$\Delta\rho_{min}$ (e Å^{-3})	−0.166	−0.183	−0.118	−0.100

Table 4 (*cont.*)

	(6) (293 K)	(6) (313 K)	(6) (338 K)	(6) (373 K)
Extinction method	None	None	None	None
Source of atomic scattering factors	*International Tables for Crystallography* (Vol. C)	*International Tables for Crystallography* (Vol. C)	*International Tables for Crystallography* (Vol. C)	*International Tables for Crystallography* (Vol. C)
Computer programs				
Data collection	*SMART* (Siemens, 1995)	*SMART* (Siemens, 1995)	*SMART* (Siemens, 1995)	*SMART* (Siemens, 1995)
Cell refinement	*SAINT* (Siemens, 1995)	*SAINT* (Siemens, 1995)	*SAINT* (Siemens, 1995)	*SAINT* (Siemens, 1995)
Data reduction	*SAINT* (Siemens, 1995)	*SAINT* (Siemens, 1995)	*SAINT* (Siemens, 1995)	*SAINT* (Siemens, 1995)
Structure solution	*SHELXS*86 (Sheldrick, 1990)	*SHELXS*86 (Sheldrick, 1990)	*SHELXS*86 (Sheldrick, 1990)	*SHELXS*86 (Sheldrick, 1990)
Structure refinement	*SHELXL*93 (Sheldrick, 1993)	*SHELXL*93 (Sheldrick, 1993)	*SHELXL*93 (Sheldrick, 1993)	*SHELXL*93 (Sheldrick, 1993)
Preparation of material for publication	*XCIF* (Sheldrick, 1993)	*XCIF* (Sheldrick, 1993)	*XCIF* (Sheldrick, 1993)	*XCIF* (Sheldrick, 1993)

decomposition at 485–487 K; the decomposition product is orange and the process probably involves the loss of HNO_3. Melting points for compounds (6) and (11) have been given in the literature (Faldt *et al.* 1997).

Elemental analyses were performed on crystals from the same batches as those used for X-ray crystallography and were generally found to give a low carbon percentage of the order of 1%. This is ascribed to difficulties associated with the combustion process of the salts. The analysis of compound (11) showed that the solvent acetonitrile molecule had been lost, consistent with the observation that the crystals are unstable in air.

2.2. *Crystallographic methods*

Experimental details are given in Tables 1–4. The crystals were mounted on glass fibres using epoxy glue, except for crystals of compound (11), which lost solvent upon exposure to the air; crystals of (11) were drawn from the mother liquor, coated with a thin layer of oil and transferred quickly to the cold nitrogen stream on the diffractometer. One of the *tert*-butyl groups of the cation of (11) was found to be disordered. This was modelled as a composite of two possible conformations for the *tert*-butyl group. Each conformation was refined with respect to the s.o.f. (site occupation factor). One of the two conformers was dominant with an s.o.f. of 0.647 (4) [the second conformer had an s.o.f of 0.353 (4)]. For compound (7), the H atom on the nitric acid molecule was found to be disordered, being present at both the NO_3 entities with an s.o.f. of one half. All 19 structures were checked for overlooked symmetry and voids using *PLATON* (Spek, 1990).†

2.3. *Dielectric measurements [of compound (6)]*

A displacement of the PF_6^- anions with respect to the cation lattice along the *c* axis would give rise to a polarization and subsequent pyroelectric or ferroelectric properties. Even though such properties are not permitted in the present space group, $R\bar{3}c$, a breaking of the symmetry by this displacement would be observed quite easily by dielectric or pyroelectric measurements, whereas it could be overseen by X-ray methods unless, of course, detailed structural knowledge is available over a large temperature span. An indication of whether paraelectric or potentially ferroelectric properties are to be expected is provided by the anisotropy and magnitudes of the components of the relative permittivity

Fig. 1. Stereoview of the cation in (6) (*ORTEP*II; Johnson 1976) that emphasizes the slight propeller shape, seen as a twist of the aromatic rings due to interactions with the hexafluorophosphate ion. (Displacement ellipsoids are plotted at the 50% probability level.)

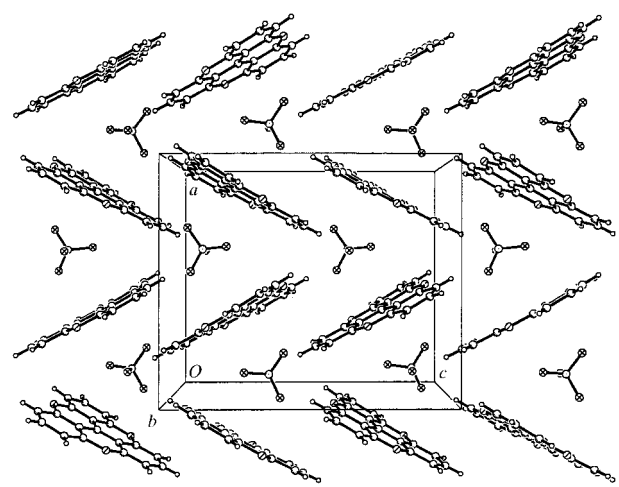

Fig. 2. The zigzag mixed stacking observed for the high space-group symmetry salts (*Pbca*), compounds (3) and (4) (*ORTEP*II; Johnson 1976). A section through the unit cell of the structure of (4) is shown here as a projection along the *b* axis.

† Supplementary data for this paper are available from the IUCr electronic archives (Reference: OS0007). Services for accessing these data are described at the back of the journal.

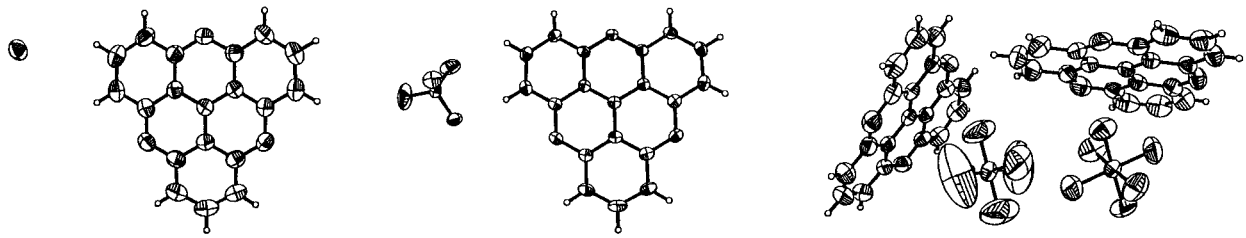

(3) (4) (5)

Fig. 3. *ORTEP*II (Johnson, 1976) drawings of the asymmetric units for the compounds (3), (4) and (5). (Displacement ellipsoids are plotted at the 50% probability level.)

tensor. The components of the tensor were found by the microwave cavity perturbation method (Buranov & Shchegolev, 1971; Ong, 1977). Five different crystals were used for the measurements. The components of the tensor were determined to be $\varepsilon_{11} = \varepsilon_{22} = 9.6 \pm 1.6$ and $\varepsilon_{33} = 5.1 \pm 1.2$, where the uncertainty represents one standard uncertainty. All other components are zero by symmetry. Spontaneous polarization on small samples is most easily determined by pyroelectric methods. The method employed was the temperature-step method (Ackermann, 1915). The setup used for pyroelectric measurements has been described in an earlier paper (Krebs *et al.* 1997). The threefold axis was found to be along the shortest dimension of the crystals, which generally had the shape of small trigonal prisms. Five different crystals were used for the measurements. Each measurement was repeated twice. No pyroelectric signal was observed in the temperature interval 293–383 K. The lack of a pyroelectric signal does not necessarily mean that there is no polarization in the material, as it could be a ferroelectric with domains of opposite polarization. Ferroelectrics can, under normal circumstances, be forced to exhibit polar properties by heating and cooling the sample in a strong electric field (poling). Poling attempts were made for crystals of (6) along the *c* axis. Electrodes were applied as for the pyroelectric measurements and the crystals were heated to 373 K in an electric field of 1–3 MV m^{-1} and cooled to ambient temperature. Attempts were made with three different crystals. Subsequent pyroelectric measurements showed no pyroelectric signal.

3. Results and discussion

The preparation of the salts followed the general procedure as indicated in the scheme above, starting from 12c-hydroxy-4,8,12-trioxa-4,8,12,12c-tetrahydrodibenzo[*cd*,*mn*]pyrene, (1) (Martin & Smith, 1964), or 2,6,10-tri(*tert*-butyl)-12c-ethoxy-4,8,12-trioxa-4,8,12,12c-tetrahydrodibenzo[*cd*,*mn*]pyrene, (2) (Faldt *et al.*, 1997; Peters, 1980), and the acid with which the salt was to be formed. General to all the salts reported was a pronounced tendency to form large well shaped crystals. Crystallographic data for the structures of compounds (3), (4), (5), (6), (7), (8), (9), (10), (11) and (12) are presented in Tables 1 and 2. Further crystallographic data for (6) at temperatures of 160, 198, 220, 243, 268, 293, 313, 338 and 373 K are presented in Tables 3 and 4. The coordinates, geometrical data and structure factors have been deposited.†

3.1. *Molecular structure*

In all the cases, the core atoms of the cations of (1) and (2) are coplanar. Bond lengths between the central C atom (position 12c) and the three aromatic C atoms to which the central atom is attached were found to be typical of an aromatic system [bond lengths in the range 1.384 (7)–1.409 (7) Å were observed]. It is, however, noticeable that for two of the compounds, namely (5) and (10), the three central C—C bond lengths differ significantly. The C—C bonds for the remaining compounds were found to have essentially the same length. This was found to correlate with the position of the anion with respect to the central C atom, being displaced towards the shorter C—C bond. The small deviations from planarity observed on the perimeter of the cation of (1) can be ascribed to crystal packing effects, as in (6) where the twist of the aromatic rings, causing the molecule to acquire a slight propeller shape, is clearly due to the interaction with the PF_6^- ion, as shown in Fig. 1.

3.2. *Cation–anion interactions*

3.2.1. *Cation–monovalent anion interactions*. The overall packing pattern of the pancake-shaped cation of (1) with an anion in the solid state was found to fall into one of two distinct categories: high point-group symmetry and low point-group symmetry. Crystals with a high point-group symmetry were observed when the anions were small and of high symmetry (I^-, BF_4^-, PF_6^-, AsF_6^-) alternating in stacks with the cation of (1). The most characteristic packing pattern is the zigzag type pattern observed for (3) and (4) (Fig. 2) and partly for (5). Compounds (3) and (4) are completely isostructural, whereas the structure of (5) has two structural motifs. One structural motif of (5) is identical to the overall

† See deposition footnote on p. 416.

motif found for (3) and (4), whereas the other structural motif is new and completely different. As the structural motifs are found in the same space group as for (3) and (4), the immediate consequence is that two different anions and two different cations are found in the asymmetric unit in (5) (Fig. 3). The second structural motif found in (5) consists of dimers of the cation of (1) with AsF_6^- anions on either side of each dimer (Fig. 4).

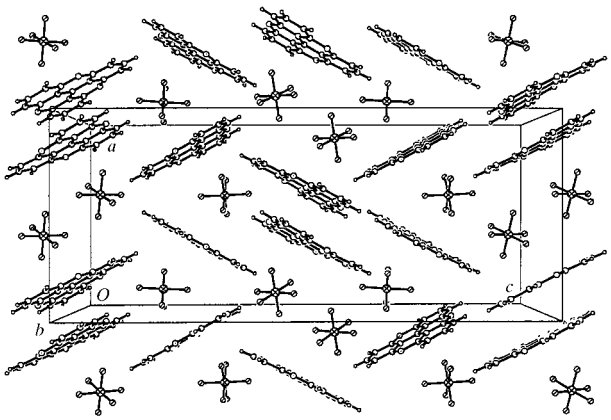

Fig. 4. A section through the unit cell showing the two structural motifs found in (5) as a projection along the *b* axis (*ORTEP*II; Johnson 1976).

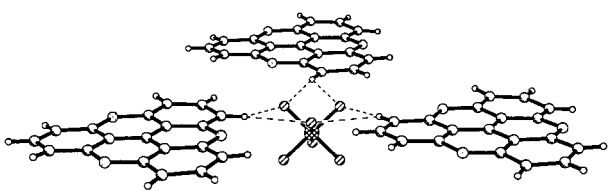

Fig. 5. A view of the interaction between the hexafluorophosphate anion and the cation in the *ab* plane of compound (6).

The difference between the two AsF_6^- anions in the asymmetric unit is quite pronounced and reflected in the As—F bond lengths and the displacement parameters of the atoms. The AsF_6^- anion found in the zigzag motif has the longest As—F bond lengths and the smallest displacement parameters. The displacement parameters of the F atoms of the AsF_6^- anion in the dimer arrangement were found to be quite high, in particular U^3/U^1 for one F atom (F12). A large anisotropy in the displacement parameters is, however, not uncommon for this type of anion, depending on the environment in the crystal. It may indicate some rotational disorder of the anion. A split-atom model was attempted but proved unsuccessful.

Interestingly, the last compound in the series of high-symmetry compounds, compound (6), crystallizes in an entirely different manner even though the anions in (5) and (6) are essentially identical with respect to charge and polarizability, albeit different in size. If the average ion-pair volume is taken as the determining factor, one finds that (3) and (4) have ion-pair volumes of 378.1 (2) and 375.8 (2) Å^3, respectively. The values for (5) and (6) are 431.0 (3) and 406.5 (1) Å^3, respectively [bearing in mind that the data for (4) and (6) were recorded at 120 K, whereas those for (3) and (5) were recorded at 293 K; for comparison, (6) at 293 K has an average ion-pair volume of 419.1 (1) Å^3]. The symmetry of the anion seems to have little or no determining influence on the packing pattern in (3), (4), (5) and (6), as all three anion symmetries, ∞, T_d, O_h, exhibit the pure zigzag pattern. The interplanar angles between the planes of the cation of (1) found within the same stack exhibiting the zigzag motif were found to be 57.1 (3), 57.8 (2) and 60.3 (5)° for (3), (4) and (5), respectively. The most likely explanation for the observed behaviour is that we are dealing with a size effect of the anion. The pure zigzag packing pattern

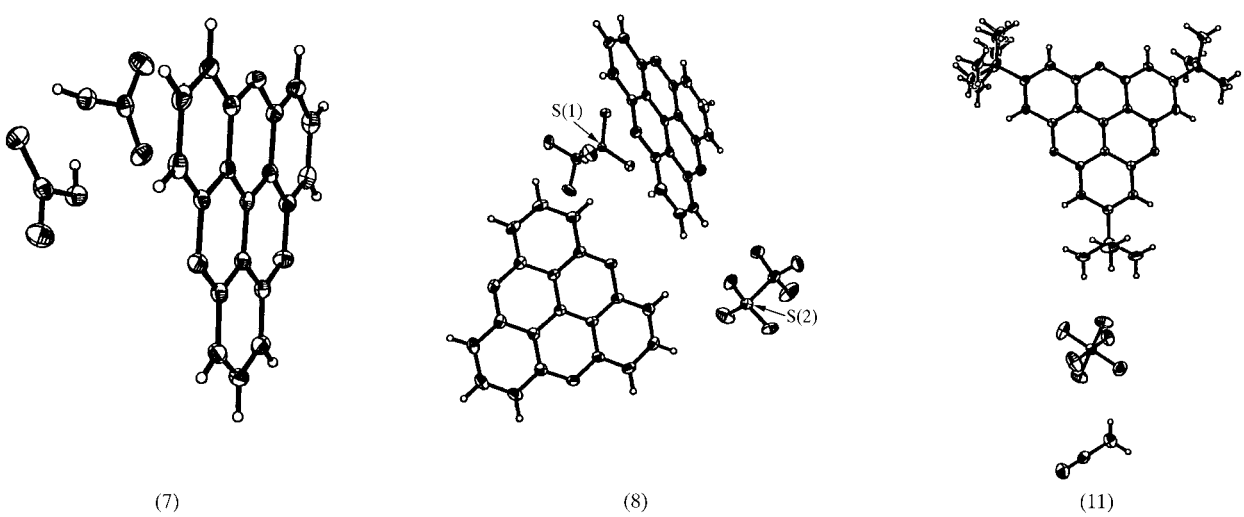

Fig. 6. *ORTEP*II (Johnson, 1976) drawings of the asymmetric units for compounds (7), (8) and (11). (Displacement ellipsoids are plotted at the 50% probability level.)

is favoured by the smaller anions. The intermediate packing pattern observed for (6) and throughout a large temperature interval is somewhat unexpected as the distance from the central atom in the anion to the central C atom is increased by a large amount when compared to the pure zigzag pattern found in (3), (4) and (5). The shortest distances found were 3.701 (5), 3.569 (3), 3.975 (8) and 4.201 (2) Å for (3), (4), (5) and (6), respectively. The large difference in distance from the anion to the central C atom in (6) can be accounted for by close contacts between the F atoms and the aromatic CH moieties, as shown in Fig. 5. The shortest aromatic C—F distance was found to be 3.363 (2) Å [F—H distance 2.692 (3) Å]. It should also be mentioned that the anion (and cation) in compound (6) is in a symmetric ionic potential (*i.e.* the distances to the anion from either side of the plane of the cation are identical). For compounds (3), (4) and (5) this is not the case.

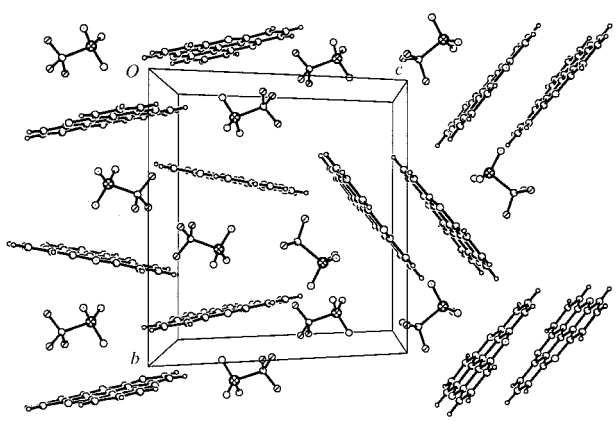

Fig. 7. Sections of the two different packing patterns observed in (8) as a projection along the *b* axis.

It was our hope that the salt (8) (Fig. 6) would be structurally related to (6); the $CF_3SO_3^-$ ion replacing the PF_6^- ion, it would, everything else being equal, lack the centre of symmetry and exhibit an exceptionally large polarization due to the large charge displacement with respect to the molecular centre in the $CF_3SO_3^-$ ion. However, low symmetry was observed with a structure not so entirely different from the structure of (5), albeit monoclinic. Compound (8) [like compound (5)] has two molecules in the asymmetric unit that are in different environments in the crystal. The ion-pair volume is, for comparison, 421.4 (2) $Å^3$. One ion pair is found in a zigzag arrangement but with a smaller interplanar angle [20.4 (1)°] compared to (3), (4) and (5). The second ion pair was found in a dimer arrangement similar to that found in (5) (Fig. 7).

The nitric acid–nitrate salt (7) was made in an attempt to incorporate anions and cations of identical symmetry; instead one molecule of nitric acid was found to co-crystallize with the nitrate anion. The structure is of low symmetry (monoclinic) and consists of stacks along the *b* axis of alternating anions and cations. The cations within each stack are coplanar but are tilted with respect to the stacking axis, forming an angle of 31.8 (1)°. The distance between the planes of the cations is 6.504 (2) Å (Fig. 8).

The effect of substituting the aromatic rings with *tert*-butyl groups, thus enlarging the size and bulkiness of the cation, as in the cation of (2), gives rise to dimers of cations with one anion on each side of the dimer. An acetonitrile solvent molecule was found to co-crystallize with the ion pair in compound (11). The plane of each

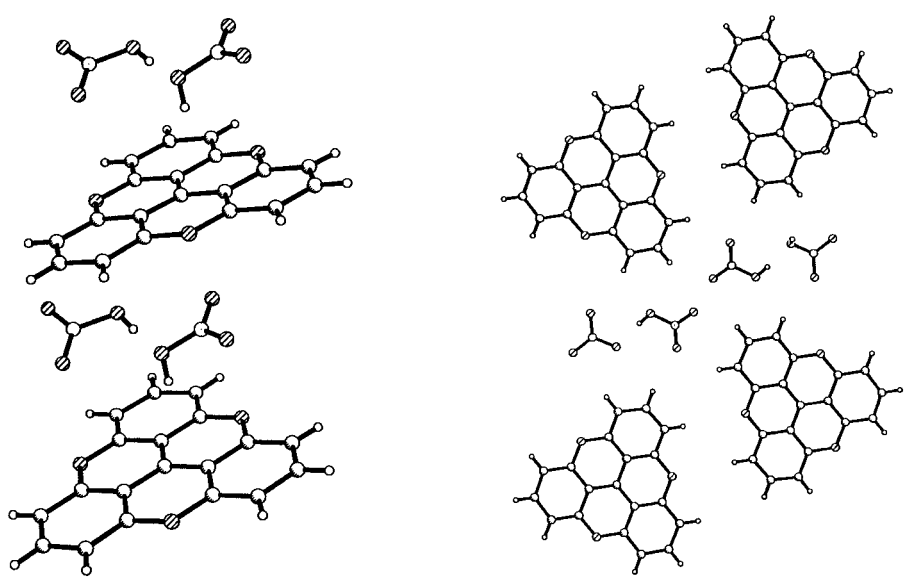

Fig. 8. (*a*) The stacks formed with nitric acid/nitrate dimers sandwiched between the cations in (7). (*b*) The interaction between the nitric acid/nitrate dimers in the plane of the anions. (The H atom associated with the nitric acid is disordered, the s.o.f. being 0.5 for each H-atom position.)

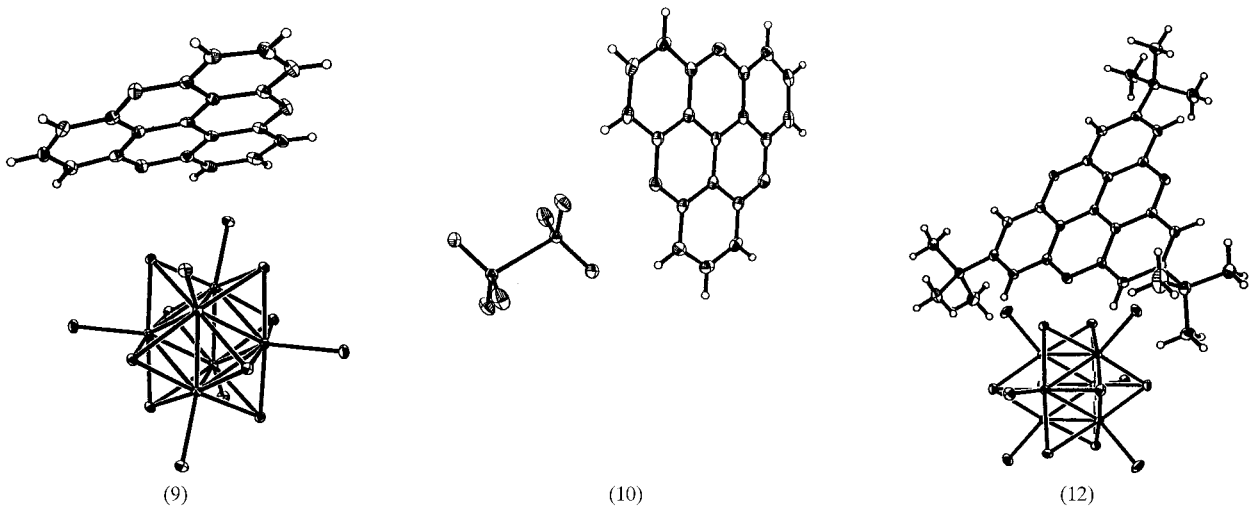

Fig. 9. *ORTEP*II (Johnson, 1976) drawings of the asymmetric units for compounds (9), (10) and (12). (Displacement ellipsoids are plotted at the 50% probability level.)

cation forms an angle of 23.3 (1)° with the *b* axis. The packing pattern is very similar to the packing pattern observed for the dimers in (5).

3.2.2. *Cation–divalent anion interactions*. The effect of having divalent anions instead of monovalent anions was explored by employing one of the few available small divalent anions $S_2O_6^{2-}$ and the readily available but rather large $Mo_6Cl_{14}^{2-}$ cluster-type divalent anion (Fig. 9). In (10), the ion-pair volume is very small [344.9 (1) Å^3] compared to those of the other compounds examined. The obvious 1:2 anion–cation stoichiometry of the system gives rise to divalent anions sandwiched between dimers of cations in triclinic symmetry (Fig. 10).

The larger cluster divalent anions seem to dominate the packing patterns with both the cation of (1) and the cation of (2) in monoclinic space groups. In (9), dimer-like aggregates of cations surround the divalent cluster anions. The planes of the cations in the aggregate form an angle of 22.8 (1)°, whereas in (12), the cations associate to form dimers, eclipsed with respect to the *tert*-butyl groups and with the planes of the cations being parallel (Fig. 11).

3.3. *Temperature study and physical properties of (6)*

3.3.1. *Thermal expansion and mean anisotropic displacements*. The thermal expansion of (6) is remarkably isotropic. The unit-cell parameters do not, however, show an entirely linear behaviour as a function of temperature (Fig. 12). There is a slight bulge on the graph in the temperature range 250–350 K. No significant changes in the intermolecular parameters were found that could account for this. The displacement parameters of (6), however, do show some slight changes within the same temperature interval. These changes are summarized in Fig. 13, where the displacement parameters of the P, F and central C atom are plotted as a function of temperature. For both P and F it is observed that the mean principal displacement with the largest magnitude changes from being in the *c* direction to being in the *a* and *b* directions upon increasing the temperature. Furthermore, the mean

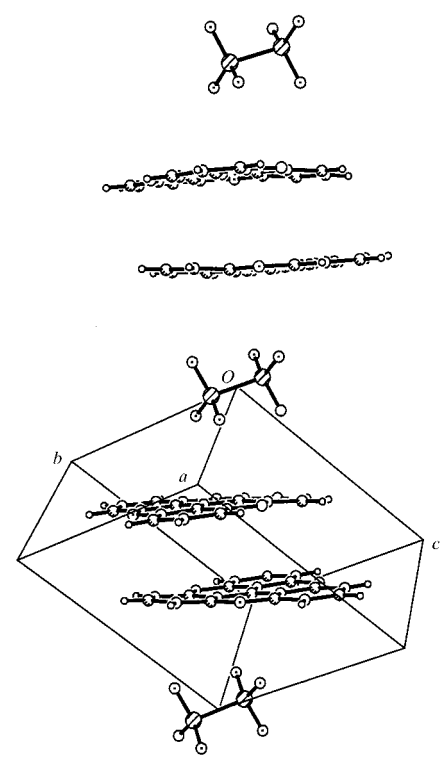

Fig. 10. The structure of (10). Stacking along the space diagonal of the triclinic unit cell is seen.

principal displacement in the *c* direction for the central C atom decreases in magnitude from 293 to 313 K.

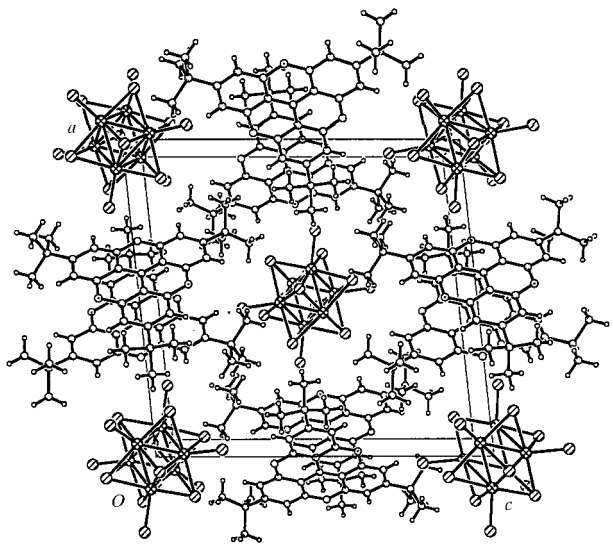

Fig. 11. A section of the structure of (12) showing the large divalent anion $Mo_6Cl_{14}^{2-}$, with the *tert*-butylated cation. A section of the structure is shown as a projection along the *b* axis, showing the packing of the cation pairs with divalent anion clusters.

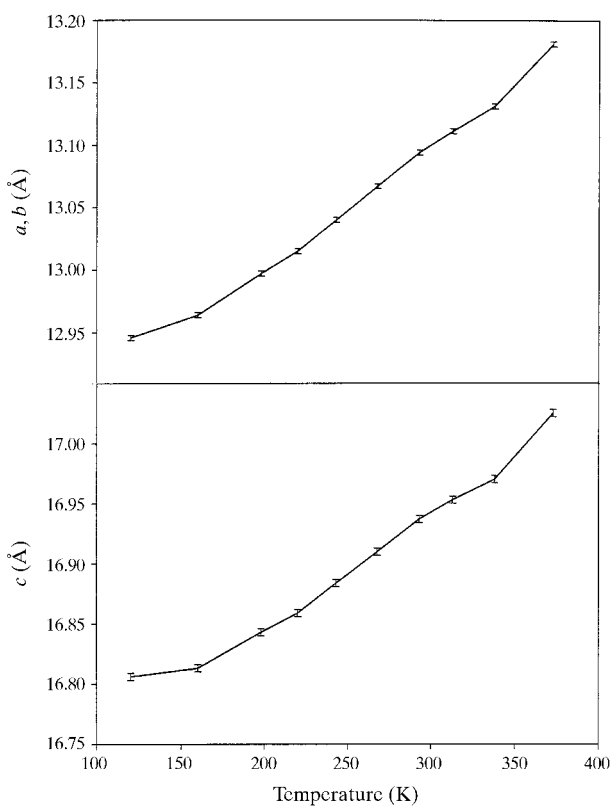

Fig. 12. Plots of the unit-cell parameters as a function of temperature for compound (6). The error bars have a length of 2σ.

The thermal appearance of (6) at the ten different temperatures is summarized in Fig. 14. As expected, the displacement parameters become quite large towards high temperature, being smallest at the central C atom and largest at the perimeter. In particular, the C atom *para* to the central C atom shows a very large mean principal displacement in the *a* and *b* directions, as shown in Fig. 15. At higher temperatures the molecule may rotate in the solid state.

3.3.2. *Dielectric properties*. The structure of compound (6) is different from all the other structures presented in this paper in the sense that it has anions and cations

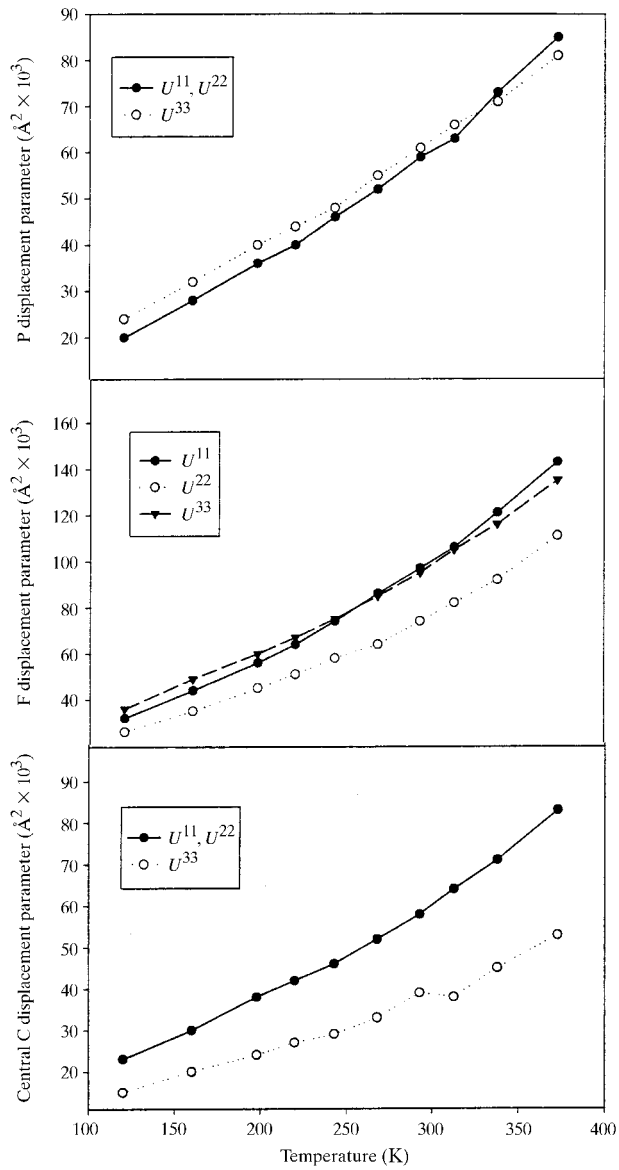

Fig. 13. The mean principal displacement parameters as a function of temperature for compound (6). The F- and P-atom graphs show crossing lines, whereas the central C atom has a region where the temperature derivative of the displacement parameter is negative.

distributed with equal interionic distances along an axis (the *c* axis). Based on the initial data collections, the noncentrosymmetric space group *R*3*c* was actually assumed, but this was later proven to be incorrect. In order to eliminate the possibility of the material becoming noncentrosymmetric in the temperature interval spanned, data were collected and the structure was determined at temperatures of 120, 160, 198, 220, 243, 268, 293, 313, 338 and 373 K. The noncentrosymmetry would be difficult to observe as only a

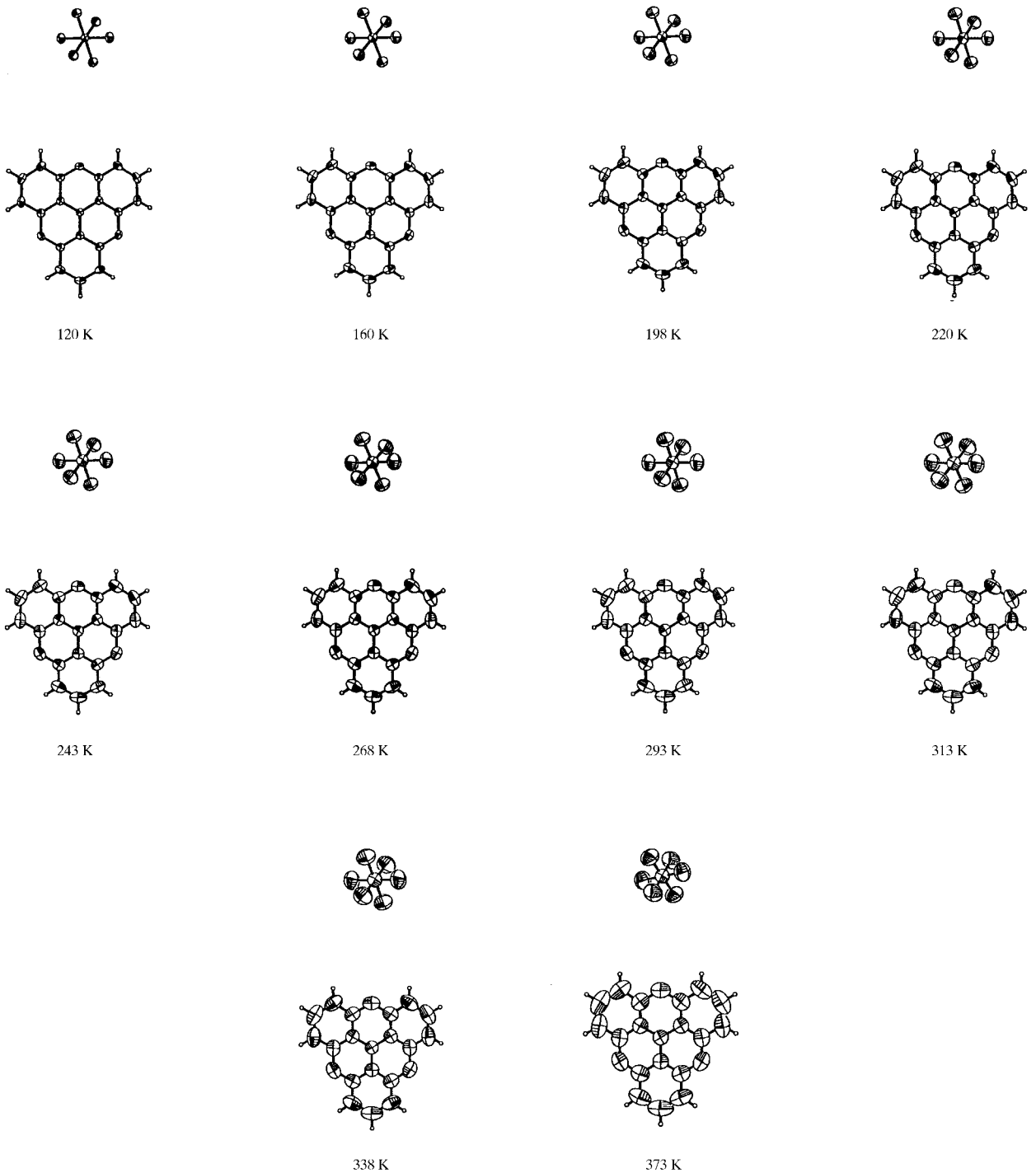

Fig. 14. The thermal evolution of (6) shown as *ORTEP*II (Johnson, 1976) drawings at the ten different temperatures at which data were collected and the structures solved. (Displacement ellipsoids are plotted at the 50% probability level.)

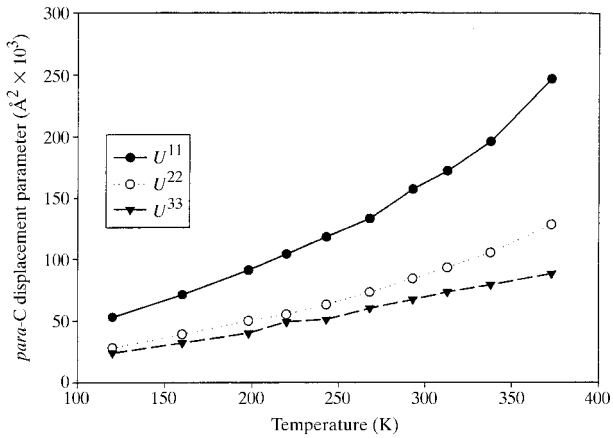

Fig. 15. The mean principal displacement parameters of the C atom at the perimeter of the system showing the largest degree of thermal motion plotted as a function of temperature.

slight displacement of the PF_6^- ion along the *c* axis would result in the reduction of the symmetry from $R\bar{3}c$ to *R*3*c*. This would result in the development of a permanent dielectric polarization and consequent pyroelectric or ferroelectric properties. No such phase transition was observed. Pyroelectric measurements confirmed this. Furthermore, the PF_6^- ion was found to be tightly bound at its site in the crystal, as evidenced by a lower polarizability along the *c* axis than along the *a* and *b* axes, as established by determination of the dielectric permittivity tensor at 35 GHz.

4. Conclusions

In conclusion, the planarity of the 4,8,12-trioxa-4,8,12,12c-tetrahydrodibenzo[*cd*,*mn*]pyrene system in the cationic state has been ascertained for ten different salts of (1) and (2) with monovalent and divalent anions. Some characteristic packing motifs depending upon the nature of the anion have been discovered and the temperature behaviour of one of the compounds has been evaluated at ten different temperatures.

References

Ackermann, W. (1915). *Ann. Phys.* **46**, 197–230.
Buranov, L. I. & Shchegolev, I. F. (1971). *Probl. Tekh. Eksp.* **2**, 171.
Faldt, A., Krebs, F. C. & Thorup, N. (1997). *J. Chem. Soc. Perkin Trans.* pp. 2219–2229.
Johnson, C. K. (1976). *ORTEP*II. Report ORNL-5138. Oak Ridge National Laboratory, Tennessee, USA.
Krebs, F. C., Larsen, P. S., Larsen, J., Jacobsen, C. S., Boutton, C. & Thorup, N. (1997). *J. Am. Chem. Soc.* **119**, 1208–1216.
Lofthagen, M., Chadha, R. & Siegel, J. S. (1991). *J. Am. Chem. Soc.* **113**, 8785–8790.
Lofthagen, M. & Siegel, J. S. (1995). *J. Org. Chem.* **60**, 2885–2890.
Lofthagen, M., VernonClark, R., Baldridge, K. K. & Siegel, J. S. (1992). *J. Org. Chem.* **57**, 61–69.
Martin, J. C. & Smith, R. G. (1964). *J. Am. Chem. Soc.* **86**, 2252–2256.
Müller, E., Moosmeyer, A., Rieker, A. & Schleffler, K. (1967). *Tetrahedron Lett.* **39**, 3877–3880.
Ong, N. P. (1977). *J. Appl. Phys.* **48**, 2935–2940.
Panico, R., Powell, W. H. & Richer, J.-C. (1993). *A Guide to IUPAC Nomenclature of Organic Compounds*. Oxford: Blackwell.
Peters, N. J. (1980). PhD dissertation, University of Illinois, USA.
Sabacky, M. J., Johnson, C. S. Jr, Smith, R. G., Gutowsky, H. S. & Martin, J. C. (1967). *J. Am. Chem. Soc.* **89**, 2054–2058.
Sheldrick, G. M. (1990). *Acta Cryst.* A**46**, 467–473.
Sheldrick, G. M. (1993). *SHELXL*93. *Program for the Refinement of Crystal Structures.* University of Göttingen, Germany.
Sheldrick, G. M. (1996). *SADABS. Empirical Absorption Program for the Siemens SMART Platform.* Siemens Analytical X-ray Instruments Inc., Madison, Wisconsin, USA.
Sheldrick, G. M. (1997). *SHELXL*97. *Program for the Refinement of Crystal Structures.* Siemens Analytical X-ray Instruments Inc., Madison, Wisconsin, USA.
Siemens (1995). *SMART* and *SAINT. Area-Detector Control and Integration Software.* Siemens Analytical X-ray Instruments Inc., Madison, Wisconsin, USA.
Spek, A. L. (1990). *Acta Cryst.* A**46**, C-34.